

Performance Improvement of LoRa Modulation with Signal Combining

The Khai Nguyen, Ha H. Nguyen, and Ebrahim Bedeer

Abstract—Low-power long-range (LoRa) modulation has been used to satisfy the low power and large coverage requirements of Internet of Things (IoT) networks. In this paper, we investigate performance improvements of LoRa modulation when a gateway is equipped with multiple antennas. We derive the optimal decision rules for both coherent and non-coherent detections when combining signals received from multiple antennas. We present expressions of the symbol/bit error probabilities of both the coherent and non-coherent detections in AWGN and Rayleigh fading channels, respectively. Moreover, we also propose an iterative semi-coherent detection that does not require any overhead to estimate the channel-state-information (CSI) while its performance can approach that of the coherent detection. Simulation and analytical results show very large power gains provided by the use of multiple antennas for all the detection schemes considered.

Index Terms—Chirp-spread spectrum modulation, LoRa, LoRaWAN, non-coherent detection, signal combining.

I. INTRODUCTION

Internet of Things (IoT) networks aim to connect a massive number of end devices (EDs) that are typically battery powered and expected to last for several years. Moreover, EDs can be deployed in geographical areas extending to several tens of kilometers and served by a few gateways [1]. Existing cellular networks can provide long range coverage but use complex modulation, coding, and multiple access techniques to deliver high data rates. As such, they are not suitable to support low power requirements of EDs that send information at much lower data rates in many IoT applications. On the other hand, wireless local-area networks (WLANs), e.g., WiFi, cannot support very large coverage.

Low-power wide-area networks (LPWANs) are emerging solutions to balance the trade-off among coverage, power requirements and data rates of IoT networks [2]. Among various solutions, low-power long-range (LoRa) technology is currently one of the most widely deployed LPWAN technologies around the world [1]. This technology is based on a proprietary chirp spread spectrum (CSS) modulation, also known as LoRa modulation, in the PHY layer and LoRaWAN protocol in the MAC layer [2], [3].

In the PHY layer, CSS operates in the ISM band (433 MHz, 868 MHz, or 915 MHz, depending on which region in the world) and encodes data symbols into chirp signals whose frequency sweeps (either increasing or decreasing over time) the entire bandwidth once. There are three main parameters in CSS, namely, coding rate, bandwidth (125, 250 or 500 kHz), and spreading factor (from 7 to 12), that can be selected to balance transmission rate, reception sensitivity, and coverage range. In the MAC layer, the LoRaWAN protocol operates in a

star topology using ALOHA multiple access. In a typical LoRa network, each ED communicates with several *single-antenna* gateways in the uplink transmission. Then, the gateways forward the received signals for each ED, the received signal strength indicator (RSSI) levels, and optional time stamps to the LoRa network server (LNS) through IP backbone. The LNS keeps the received message with the highest RSSI and drops the rest. For downlink transmission to a specific ED, the LNS picks a gateway having the highest RSSI from that ED.

It is pointed out that all research works on LoRa modulation consider that gateways are equipped with a single antenna. For example, the authors in [4] analyze the bit error rate (BER) performance of LoRa modulation and provided tight closed-form approximations in both additive white Gaussian noise (AWGN) and Rayleigh fading channels. In [5], the authors introduce a slope-shift-keying LoRa scheme that increases the achievable bit rate of the conventional LoRa system by adding a down chirp and its cyclic shifts. The authors also develop low-complexity optimum coherent and non-coherent detectors, as well as, tight approximations for BER and symbol error rate (SER) when the non-coherent detector is employed in the presence of Rayleigh fading channels. In [6], the authors investigate performance of LoRa in the presence of interference from another LoRa user that is neither chip nor phase aligned with the LoRa signal of the desired user. They derive expressions for SER and frame error rates. In [7], the authors exploit index modulation to further improve the data rates of conventional CSS systems and derive optimal detection rules for both coherent and non-coherent detections. Further, they propose a low-complexity non-coherent detection scheme whose performance approaches the optimal performance.

Given the widespread use of multiple antennas in wireless communication systems, it is well expected that gateways in LoRa systems are fitted with multiple antennas. As such, it is natural and useful to evaluate the BER performance of a LoRa system equipped with *multiple-antenna* gateways and quantify the performance gain over the system using *single-antenna* gateways. This is precisely the objective of this paper. Specifically, we first explain how multiple received signals at the gateway are combined under both cases of coherent and non-coherent detection. We then present the BER expressions for coherent detection in AWGN channels and for non-coherent detection in Rayleigh fading channels. Moreover, we propose a novel iterative semi-coherent detection that can blindly estimate the CSI, i.e., without any training overhead, and significantly outperform the non-coherent detection, especially when the number of antennas at the gateway increases. The obtained results show that proper combining multiple received signals at the gateway can significantly improve the LoRa modulation performance, which results in either power saving of EDs, or extended coverage.

The authors are with the Department of Electrical and Computer Engineering, University of Saskatchewan, Saskatoon, Canada S7N5A9. Emails: {khai.nguyen, ha.nguyen, e.bedeer}@usask.ca.

II. SYSTEM MODEL

We consider the uplink transmission of a LoRa network where each ED communicates with a gateway equipped with L antennas¹. One LoRa symbol has a bandwidth B and duration T_{sym} . Let $T_s = 1/B$ be the sampling period. Then each LoRa symbol can be represented by $M = T_{\text{sym}}/T_s = 2^{\text{SF}}$ samples, where $\text{SF} \in \{7, 8, \dots, 12\}$ is the spreading factor, which is also the number of information bits encoded into one LoRa symbol. Let f_c be the carrier frequency. Then the operating frequency range $[f_c - B/2, f_c + B/2]$ is divided into M equally-spaced frequency bins, and each LoRa symbol (i.e., a chirp signal) starts at an initial frequency belonging to one of the M frequency bins, and linearly increases/decreases until it reaches the maximum frequency $f_c + B/2$. Then, it is folded to $f_c - B/2$ and continues to increase/decrease until the end of the symbol duration T_{sym} . It can be shown that LoRa modulation is M -ary orthogonal modulation [8].

The baseband discrete-time basic up chirp (of length M samples) is given as [5]:

$$x_0[n] = A \exp\left(j2\pi\left(\frac{n^2}{2M} - \frac{n}{2}\right)\right), n = 0, 1, \dots, M-1. \quad (1)$$

Then, the set of M orthogonal chirps can be simply constructed from $x_0[n]$ as $x_m[n] = x_0[n+m]$, $m = 0, 1, \dots, M$. With the sampling period of $T_s = T_{\text{sym}}/M$, the equivalent analog (continuous-time) chirps have an equal energy of $E_s = \int_0^{T_{\text{sym}}} |x_0(t)|^2 dt = \left(\sum_0^{M-1} |x_0[n]|^2\right) T_s = A^2 T_{\text{sym}}$. It also follows that the signal power is $P_{\text{signal}} = \frac{E_s}{T_{\text{sym}}} = A^2$.

We consider a frequency-flat and slow Rayleigh fading channel between each ED and each receive antenna. With such a channel model, the received signal at the ℓ th antenna of the gateway is given as

$$y_\ell[n] = h_\ell x_m[n] + w_\ell[n] = \alpha_\ell \exp(j\theta_\ell) x_m[n] + w_\ell[n], \quad (2)$$

where $w_\ell[n] \sim \mathcal{CN}(0, \sigma^2)$ is a zero-mean AWGN sample at the ℓ th antenna, $h_\ell = \alpha_\ell \exp(j\theta_\ell)$ represents the complex channel coefficient (in which α_ℓ denotes the channel's attenuation and θ_ℓ represents the phase shift). For the Rayleigh fading channel, α_ℓ follows a Rayleigh distribution with average power gain of 1, i.e., $\mathbb{E}\{|\alpha_\ell|^2\} = 1$, whereas θ_ℓ is uniformly distributed over $[0, 2\pi]$. Note also that the case of an AWGN channel corresponds to setting $\alpha_\ell = 1$ and $\theta_\ell = 0$, $\forall \ell$.

Before closing this section, it is important to comment on the signal-to-noise ratio (SNR) relevant to the considered system model. Using the standard notation of N_0 for the one-sided power spectral density of additive white Gaussian noise, the noise power inside the signal bandwidth B is simply $P_{\text{noise}} = N_0 B$, which is also precisely the variance σ^2 of the AWGN sample $w_\ell[n]$ in (2). It then follows that the average SNR at each receive antenna, denoted as $\overline{\text{SNR}}$ is given as $\overline{\text{SNR}} = \frac{P_{\text{signal}}}{P_{\text{noise}}} = \frac{E_s/T_{\text{sym}}}{N_0 B} = \frac{E_s/M}{N_0}$. This $\overline{\text{SNR}}$ is exactly the same as A^2/σ^2 calculated based on the discrete-time baseband model in (2), which should be. In Section VI, all the analytical and simulated BER curves are plotted versus this $\overline{\text{SNR}}$.

¹The techniques and results in this paper are also applicable when combining signals received from different single-antenna gateways.

III. COHERENT DETECTION OVER AWGN CHANNELS

In coherent detection, perfect knowledge of the CSI is assumed and used to perform the maximal ratio combining (MRC) of L received signal. Specifically, the received signal at the ℓ th antenna is first correlated with the complex conjugate of the respective channel coefficient as follows:

$$v_\ell^{(\text{coh})}[n] = h_\ell^* y_\ell[n] = \alpha_\ell^2 x_m[n] + \hat{w}_\ell[n], \quad l = 1, \dots, L, \quad (3)$$

where $\hat{w}_\ell[n] \sim \mathcal{CN}(0, \alpha_\ell^2 \sigma^2)$. The received signal after the MRC is given as

$$r[n] = \sum_{l=1}^L v_\ell^{(\text{coh})}[n] = \left(\sum_{l=1}^L \alpha_\ell^2\right) x_m[n] + \hat{w}[n], \quad (4)$$

where $\hat{w}[n] \sim \mathcal{CN}\left(0, \sigma^2 \sum_{l=1}^L \alpha_\ell^2\right)$.

To demodulate the combined signal $r[n]$, we perform normalizing and dechirping, i.e., multiplying $r[n]$ with the scaled conjugate of the basic chirp $x_0[n]$ as follows

$$\begin{aligned} z[n] &= \frac{r[n] x_0^*[n]}{\sqrt{\sum_{l=1}^L \alpha_\ell^2}} \frac{A}{A} \\ &= \underbrace{\beta A \exp\left(j2\pi\left(\frac{m^2}{2M} - \frac{m}{2}\right)\right)}_{\text{constant phase } \Psi_m} \underbrace{\exp\left(\frac{j2\pi mn}{M}\right)}_{\text{linear phase}} + \bar{w}[n], \end{aligned} \quad (5)$$

where $\bar{w}[n] \sim \mathcal{CN}(0, \sigma^2)$ and $\beta = \sqrt{\sum_{l=1}^L \alpha_\ell^2}$ is the effective gain due to MRC. Then, we perform the M -point FFT on the dechirped signal $z[n]$ as

$$\begin{aligned} Z^{(\text{coh})}[k] &= \frac{1}{\sqrt{M}} \sum_{n=0}^{M-1} z[n] \exp\left(\frac{-j2\pi nk}{M}\right) \\ &= \frac{1}{\sqrt{M}} \sum_{n=0}^{M-1} \left(\beta A \exp(j\pi \Psi_m) \exp\left(\frac{j2\pi mn}{M}\right) + \bar{w}[n]\right) \\ &= \begin{cases} \beta A \sqrt{M} \exp(j\pi \Psi_m) + W[m], & k = m \\ W[k], & k = 1, \dots, M, k \neq m, \end{cases} \end{aligned} \quad (6)$$

where $W[\cdot] \sim \mathcal{CN}(0, \sigma^2)$ is the noise sample after the FFT. One can see from (5) that the phase Ψ_m is deterministic, hence, the equivalent decision variable can be re-written as

$$\begin{aligned} Z_R^{(\text{coh})}[k] &= \Re\left\{Z^{(\text{coh})}[k] \exp(-j\Psi_m)\right\} \\ &= \begin{cases} \beta A \sqrt{M} + W_R[m], & k = m \\ W_R[k], & k = 1, \dots, M, k \neq m, \end{cases} \end{aligned} \quad (7)$$

where $\Re\{\cdot\}$ returns the real value and $W_R[\cdot] \sim \mathcal{CN}(0, \sigma^2/2)$. For ease in performance analysis, we scale the decision variable in (7) by \sqrt{B} to obtain $\hat{Z}_R^{(\text{coh})}[k] = Z_R^{(\text{coh})}[k]/\sqrt{B}$. Using the relationships $E_s = A^2 T_{\text{sym}} = A^2 M/B$ and $\sigma^2 = N_0 B$, the scaled decision variable is expressed as

$$\hat{Z}_R^{(\text{coh})}[k] = \begin{cases} \beta \sqrt{E_s} + \hat{W}_R[m], & k = m \\ \hat{W}_R[k], & k = 1, \dots, M, k \neq m, \end{cases} \quad (8)$$

where $\hat{W}_R[\cdot] \sim \mathcal{CN}(0, N_0/2)$. Finally, the decision rule is given as

$$\hat{m}^{(\text{coh})} = \arg \max_{k=0,1,\dots,M-1} \hat{Z}_R^{(\text{coh})}[k]. \quad (9)$$

Coherent detection is not very practical for fading channels since it needs precise channel estimation (which typically comes with extra training overhead and complexity). As such, we complete this section by presenting the error probability of LoRa modulation with MRC in AWGN channels, i.e., when $\alpha_\ell = 1$ and $\theta_\ell = 0$, and $\beta = \sqrt{L}$. One can observe that the decision variable in (8) is the same as that for orthogonal M -ary FSK. Therefore, the error probability of LoRa modulation with the maximum-ratio combining of L signals is the same as in the single antenna case for orthogonal modulations, except with a power gain of L due to the MRC. Accordingly, the symbol error probability for the LoRa modulation can be obtained by replacing E_s with LE_s in the symbol error probability of M -ary FSK using a single antenna [9, equation 8.67]. This yields

$$P_s^{(\text{coh})} = 1 - \frac{1}{\sqrt{2\pi}} \int_{-\infty}^{\infty} \left(\frac{1}{\sqrt{2\pi}} \int_{-\infty}^y \exp\left(-\frac{x^2}{2}\right) dx \right)^{M-1} \times \exp\left(-\frac{1}{2} \left(y - \sqrt{\frac{2LE_s}{N_0}} \right)^2\right) dy. \quad (10)$$

Finally, the bit error probability of LoRa modulation in AWGN channels with MRC can be found as $P_b^{(\text{coh})} = \frac{M}{2(M-1)} P_s^{(\text{coh})}$.

IV. NON-COHERENT DETECTION OVER FADING CHANNELS

As mentioned before, precise knowledge of the CSI requires complex signal processing that may not be suitable for IoT networks. As such, non-coherent detection of LoRa modulation is much more relevant and that's why it is implemented in practical systems. The first step in the non-coherent detection of LoRa modulation is to perform normalizing and dechirping of the received signal at the ℓ th antenna in (2) as follows

$$v_\ell^{(\text{non-coh})}[n] = y_\ell[n] \frac{x_0^*[n]}{A}, \\ = \alpha_\ell \exp(j\theta_\ell) A \exp(j\Psi_m) \exp\left(\frac{j2\pi mn}{M}\right) + \bar{w}_\ell[n], \quad (11)$$

where $\bar{w}_\ell[n] \sim \mathcal{CN}(0, \sigma^2)$. Then by performing the M -point FFT on the dechirped signal $v_\ell^{(\text{non-coh})}[n]$ and dividing the result by \sqrt{B} , we obtain

$$V_\ell[k] = \begin{cases} \sqrt{E_s} \alpha_\ell \exp(j\theta_\ell) \exp(j\pi\Psi_m) + W_\ell[m], & k = m \\ W_\ell[k], & k = 1, \dots, M, k \neq m \end{cases} \\ = \begin{cases} \sqrt{E_s} a_\ell[m] + W_\ell[m], & k = 1, \dots, M, k = m \\ W_\ell[k], & \text{otherwise,} \end{cases} \quad (12)$$

where $a_\ell[k] = \alpha_\ell \exp\{j\theta_\ell\} \exp\{j\pi\Psi_k\} = h_\ell \exp\{j\pi\Psi_k\} \sim \mathcal{CN}(0, 1)$ and $W_\ell[k] \sim \mathcal{CN}(0, N_0)$.

Since CSI is not available in non-coherent detection, we apply the square-law combining to all the received signals from the L antennas at bin k as

$$Z^{(\text{non-coh})}[k] = \sum_{l=1}^L |V_\ell[k]|^2 \\ = \begin{cases} \sum_{l=1}^L |\sqrt{E_s} a_\ell[m] + W_\ell[m]|^2, & k = m \\ \sum_{l=1}^L |W_\ell[k]|^2, & \text{otherwise.} \end{cases} \quad (13)$$

Then, the final decision rule can be expressed as

$$\hat{m}^{(\text{non-coh})} = \arg \max_{k=0,1,\dots,M-1} Z^{(\text{non-coh})}[k]. \quad (14)$$

To find the error probability for the non-coherent detection of LoRa modulation, we follow a similar analysis as in [10]. Without loss of generality, if we assume $x_0[n]$ was transmitted, then the square-law combining output at the 0th bin is $\Lambda_0 = Z^{(\text{non-coh})}[0] = \sum_{l=1}^L |\sqrt{E_s} a_\ell[0] + W_\ell[0]|^2$, whereas the output at bin k , $\forall k, k \neq 0$ is $\Lambda_k = Z^{(\text{non-coh})}[k] = \sum_{l=1}^L |W_\ell[k]|^2$. To calculate the probability of error, we need first to find the probability that $\Lambda_0 > \Lambda_k, \forall k, k \neq 0$. One can show that $\Lambda_k, \forall k$, are mutually statistically independent random variables. Hence,

$$P(\Lambda_1 < \Lambda_0, \Lambda_2 < \Lambda_0, \dots, \Lambda_{M-1} < \Lambda_0) \\ = (P(\Lambda_1 < \Lambda_0))^{M-1} = \left(\int_0^{\lambda_0} f(\lambda_1) d\lambda_1 \right)^{M-1} \\ = \left(1 - \exp\left(-\frac{\lambda_0}{\sigma_1^2}\right) \sum_{q=0}^{L-1} \frac{1}{q!} \left(\frac{\lambda_0}{\sigma_1^2}\right)^q \right)^{M-1}, \quad (15)$$

where $f(\lambda_1)$ is the probability density function of Λ_1 , given as

$$f(\lambda_1) = \frac{1}{(\sigma_1^2)^L (L-1)!} \lambda_1^{L-1} \exp\left(-\frac{\lambda_1}{\sigma_1^2}\right), \quad (16)$$

and $\sigma_1^2 = \mathbb{E}\{|W_\ell[k]|^2\} = N_0$. The probability of a correct symbol decision can be calculated by averaging (15) over the probability density function of Λ_0 , which is

$$f(\lambda_0) = \frac{1}{(\sigma_0^2)^L (L-1)!} \lambda_0^{L-1} \exp\left(-\frac{\lambda_0}{\sigma_0^2}\right), \quad (17)$$

where $\sigma_0^2 = \mathbb{E}\{|\sqrt{E_s} a_\ell[m] + W_\ell[0]|^2\} = E_s + N_0$. Then, the probability of symbol error equals 1 minus the probability of a correct symbol decision and is given as [10, equation 14.4–47]

$$P_s^{(\text{non-coh})} = 1 - \int_0^\infty \frac{1}{(\sigma_0^2)^L (L-1)!} \lambda_0^{L-1} \exp\left(-\frac{\lambda_0}{\sigma_0^2}\right) \\ \times \left(1 - \exp\left(-\frac{\lambda_0}{\sigma_1^2}\right) \sum_{q=0}^{L-1} \frac{1}{q!} \left(\frac{\lambda_0}{\sigma_1^2}\right)^q \right)^{M-1} d\lambda_0 \\ = 1 - \int_0^\infty \frac{1}{(1 + \bar{\gamma}_c)^L (L-1)!} \lambda_0^{L-1} \exp\left(-\frac{\lambda_0}{1 + \bar{\gamma}_c}\right) \\ \times \left(1 - \exp(-\lambda_0) \sum_{q=0}^{L-1} \frac{\lambda_0^q}{q!} \right)^{M-1} d\lambda_0, \quad (18)$$

where $\bar{\gamma}_c = E_s/N_0 = M \cdot \overline{\text{SNR}}$. It is pointed out that (18) can be written in a closed-form finite sum as in [10, equation 14.4–49]. However, such an expression is hard to compute for high values of M and L as in the case of LoRa modulation considered in this paper. In Section VI, we evaluate (18) directly using numerical integration.

Finally, the bit error probability of non-coherent detection of LoRa modulation with signal combining is given as $P_b^{(\text{non-coh})} = \frac{M}{2(M-1)} P_s^{(\text{non-coh})}$

V. PROPOSED SEMI-COHERENT DETECTION

In this section, we propose an iterative *semi-coherent* detector for LoRa modulation when combining L received signals without needing extra overhead for CSI estimation. Section VI shows that the error performance of the proposed detector can closely approach that of the coherent detector.

Observe from (12) that if the detection of the first LoRa symbol is correct, a least-square (LS) estimate of the channel coefficient h_ℓ can be obtained as $\hat{h}_\ell = V_\ell[\hat{m}_1] \exp\{-j\pi\Psi_{\hat{m}_1}\}/\sqrt{E_s}$, where \hat{m}_1 is the detected value of the first LoRa symbol. Then, for the detection of each subsequent LoRa symbol, instead of the square-law combining in (13), we use $\hat{a}_\ell[k] = \hat{h}_\ell \exp\{j\pi\Psi_k\}$ to co-phase $V_\ell[k]$ before coherently combining (adding) the signals received from all L antennas. Mathematically, the decision variable for the proposed semi-coherent detection is

$$Z^{(\text{semi-coh})}[k] = \sum_{l=1}^L (\hat{a}_\ell[k])^* V_\ell[k], \quad (19)$$

and the final decision rule can be expressed as

$$\hat{m}^{(\text{semi-coh})} = \arg \max_{k=0,1,\dots,M-1} \Re\{Z^{(\text{semi-coh})}[k]\}. \quad (20)$$

There are two important observations regarding the above semi-coherent detection. First, since the decision rule in (20) is obtained by finding the maximum of $\Re\{Z^{(\text{semi-coh})}[k]\}$, it is invariant to the scaling of the channel estimate \hat{h}_ℓ . As such, one can simply use $\hat{h}_\ell = V_\ell[\hat{m}_1] \exp\{-j\pi\Psi_{\hat{m}_1}\}$ for the combining operation in (19). Second, the performance of the above semi-coherent is strongly influenced by the detection of the first LoRa symbol, \hat{m}_1 . If the first LoRa symbol is not detected correctly, the channel is estimated using a wrong bin, and hence contains only noise. To address this issue, we propose to perform average channel estimate and iterative estimation and detection as follows.

Assume that the fading channels stay constant for a coherence time of τ_c LoRa symbols. In the first stage, initial detection of τ_c LoRa symbols is carried out using the non-coherent detector in (14). Let $\hat{\mathbf{m}} = [\hat{m}_1, \dots, \hat{m}_{\tau_c}]$ be a vector containing these initial detected LoRa symbols. For the i th symbol, let $V_{\ell,i}[\hat{m}_i]$ denote the FFT value at the \hat{m}_i th bin. Then, the ℓ th channel coefficient is estimated as $\hat{h}_{\ell,i} = V_\ell[\hat{m}_i] \exp\{-j\pi\Psi_{\hat{m}_i}\}$ and the average channel estimate is obtained as

$$\hat{h}_\ell^{(\text{ave})} = \frac{1}{\tau_c} \sum_{i=1}^{\tau_c} \hat{h}_{\ell,i} = \frac{1}{\tau_c} \sum_{i=1}^{\tau_c} V_\ell[\hat{m}_i] \exp\{-j\pi\Psi_{\hat{m}_i}\}. \quad (21)$$

Note that, because the noise $W_{\ell,i}[m]$ are independent from symbol to symbol, when the coherent time goes to infinity, we can achieve the exact (scaled) channel value, i.e., $\hat{h}_\ell^{(\text{ave})} \xrightarrow[\tau_c \rightarrow \infty]{\text{a.s.}} \sqrt{E_s} h_\ell$.

In the second stage, we use $\hat{a}_\ell^{(\text{ave})}[k] = \hat{h}_\ell^{(\text{ave})} \exp\{j\pi\Psi_k\}$ to combine L signals from the antenna array in a similar manner as in (19) and perform new detection of all τ_c LoRa symbols as in (20). After this new detection operation, a new average channel estimate is obtained, while the newly detected

LoRa symbols are saved and compared to the previously-detected results. The iteration process between detection and estimation continues until convergence, i.e., when the detected symbols in two consecutive iterations are the same. When operating at low SNRs, the iterative semi-coherent detector does not likely to converge because the initial non-coherent detection is not reliable and the channel estimation is largely based on the wrong frequency bins. In such a case, we use a predetermined number of iterations as a stopping criterion.

The proposed iterative semi-coherent detection algorithm is summarized in Algorithm 1.

Algorithm 1 Iterative semi-coherent detection

Require: Spreading factor (SF), τ_c , N_{\max} .

- 1: Initially detect τ_c symbols $\hat{\mathbf{m}} = [\hat{m}_1, \dots, \hat{m}_{\tau_c}]$ with non-coherent detection.
 - 2: Estimate $\hat{h}_{\ell,i}$ corresponding to τ_c detected LoRa symbols ($i = 1, 2, \dots, \tau_c$).
 - 3: Obtain the average channel estimate $\hat{h}_\ell^{(\text{ave})}$ as in (21).
 - 4: Save current decision as $\hat{\mathbf{m}}_{\text{prev}} = \hat{\mathbf{m}}$.
 - 5: flag = 1; count = 0;
 - 6: **while** flag = 1 & count $\leq N_{\max}$ **do**
 - 7: count = count + 1;
 - 8: For the i th symbol, combine $V_{\ell,i}[k]$ with $\hat{a}_\ell^{(\text{ave})}[k] = \hat{h}_\ell^{(\text{ave})} \exp\{j\pi\Psi_k\}$ as in (19) and perform a new detection of the i th symbol \hat{m}_i as in (20), $\forall i = 1, 2, \dots, \tau_c$.
 - 9: Update $\hat{h}_\ell^{(\text{ave})}$ using newly detected symbols $\hat{\mathbf{m}}$.
 - 10: **if** $\hat{\mathbf{m}}_{\text{prev}} \neq \hat{\mathbf{m}}$ **then**
 - 11: flag = 1
 - 12: **else**
 - 13: flag = 0
 - 14: **end if**
 - 15: $\hat{\mathbf{m}}_{\text{prev}} = \hat{\mathbf{m}}$
 - 16: **end while**
 - 17: **return** $\hat{\mathbf{m}}$.
-

VI. RESULTS AND DISCUSSION

In this section, we provide numerical results for the BER of both coherent detection in an AWGN channel and non-coherent detection in a Rayleigh fading channel to validate our theoretical analysis. We also show the BER performance of the proposed iterative semi-coherent detection. A minimum of 10^5 Monte-Carlo trails were used to generate the BER curves for the detectors under study and the maximum number of iterations of the semi-coherent detection is set to 50. For the Rayleigh channel, it is assumed to be frequency flat and stays constant over the duration of $\tau_c = 10$ LoRa symbols.

Fig. 1 plots the simulated and theoretical BER curves of both coherent detection in AWGN channels and non-coherent detection in Rayleigh fading channels versus the average received signal-to-noise ratio per antenna, i.e., $\overline{\text{SNR}}$ (defined at the end of Section II) and for SF = 10. As one can observe, the simulated BER results of both detection techniques match perfectly with the theoretical results. As expected, increasing the number of antennas at the gateway helps to improve the BER performance. In particular, for a BER of 10^{-4} , increasing the number of antennas from $L = 1$ to 4 results in approximately 8 and 29 dB savings in the SNR (i.e., the transmit power) for the coherent and non-coherent detection cases, respectively. These numbers represent a tremendous performance improvement of both detectors, especially the non-coherent detector that does not require CSI knowledge.

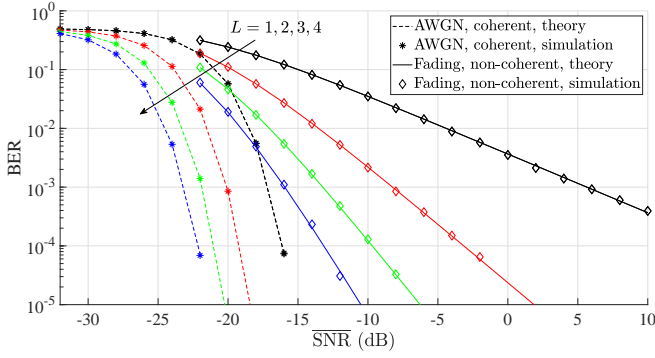


Fig. 1. BERs of coherent detection in an AWGN channel and non-coherent detection in a Rayleigh fading channel: SF = 10 and $L = 1, 2, 3, 4$.

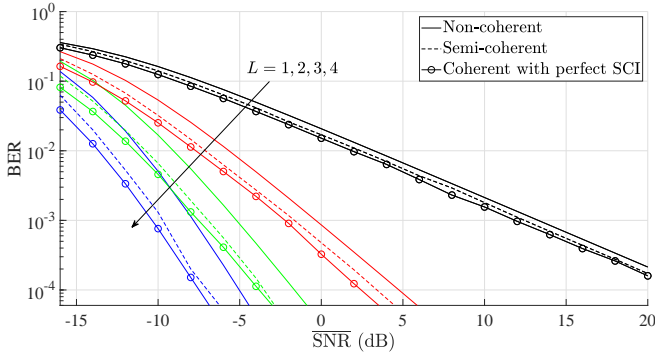


Fig. 2. BER performance comparison among the coherent detection, non-coherent detection, and semi-coherent detection in Rayleigh fading channels for SF = 7, $\tau_c = 10$, and $L = 1, 2, 3, 4$.

Fig. 2 compares the BER performance of the non-coherent (by theory), semi-coherent (by simulation), and coherent detection (by simulation) versus SNR over Rayleigh fading channels for SF = 7 and $\tau_c = 10$. It is emphasized that the performance of the coherent detection is obtained with perfect CSI knowledge, whereas CSI is not needed in the non-coherent detection and it is *blindly* estimated (i.e., without any training information) in the proposed iterative semi-coherent detection. One can see that the iterative semi-coherent detection performs within a fraction of dB from the coherent detection. Also, one can observe that properly combining the received signals from multiple antennas provides similar SNR gains as in the cases of non-coherent and coherent detections. Such results clearly show the promise of using the proposed iterative semi-coherent detection in LoRa modulation with signal combining.

Finally, Fig. 3 depicts the influence of the coherence time on the BER performance of the proposed semi-coherent detection over a Rayleigh fading channel for SF = 7, $L = 4$ and three different values of coherence time, namely, $\tau_c = 5, 10, 20$ LoRa symbols. As expected, as the channels change slower, i.e., when the coherence time is larger, the blind channel estimate becomes more accurate, and hence the performance of the proposed semi-coherent detection approaches closer to that of the coherent detection. For the worst situation considered, i.e., when $\tau_c = 5$, the semi-coherent detection can still provide an impressive SNR gain of more than 1 dB over the non-coherent detection.

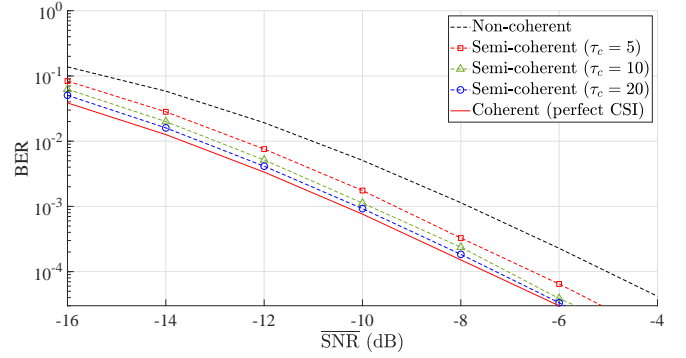


Fig. 3. Effect of coherence time on the performance of the proposed semi-coherent detection.

VII. CONCLUSION

We have investigated performance improvements of LoRa modulation when multiple antennas are employed at the gateway and by combining signals received over these antennas. The optimal decision rules were established and the corresponding BER expressions were obtained for both coherent and non-coherent detections in AWGN and Rayleigh fading channels, respectively. More importantly, we also proposed an iterative semi-coherent detection whose performance approaches that of the coherent detection without the need to spend extra resources for CSI training or estimation. Simulation results showed that increasing the number of antennas at the gateway from 1 to 4 results in approximately 8 and 29 dB savings in the transmit power of the end devices when the system operates over AWGN and Rayleigh fading channels, respectively. The results revealed that the semi-coherent detection performs within a fraction of dB from the coherent detection. As a future work, it would be useful to perform theoretical performance analysis of the proposed semi-coherent detection of LoRa signals.

REFERENCES

- [1] M. Centenaro, L. Vangelista, A. Zanella, and M. Zorzi, "Long-range communications in unlicensed bands: The rising stars in the IoT and smart city scenarios," *IEEE Wireless Commun.*, vol. 23, pp. 60–67, Oct. 2016.
- [2] Z. Qin, F. Y. Li, G. Y. Li, J. A. McCann, and Q. Ni, "Low-power wide-area networks for sustainable IoT," *IEEE Wirel. Commun.*, vol. 26, pp. 140–145, June 2019.
- [3] B. Reynders and S. Pollin, "Chirp spread spectrum as a modulation technique for long range communication," in *IEEE Symp. on Commun. and Veh. Technol.*, pp. 1–5, Nov. 2016.
- [4] T. Elshabrawy and J. Robert, "Closed-form approximation of LoRa modulation BER performance," *IEEE Commun. Letters*, vol. 22, pp. 1778–1781, Sept. 2018.
- [5] M. Hanif and H. H. Nguyen, "Slope-shift keying LoRa-based modulation," *IEEE Internet Things J.*, vol. 8, pp. 211–221, Jan. 2021.
- [6] O. Afisiadis, M. Cotting, A. Burg, and A. Balatsoukas-Stimming, "On the error rate of the LoRa modulation with interference," *IEEE Trans. on Wireless Commun.*, vol. 19, pp. 1292–1304, Feb. 2020.
- [7] M. Hanif and H. H. Nguyen, "Frequency-shift chirp spread spectrum communications with index modulation," [Online]. Available: arXiv:2102.04642v1 [cs.IT], Feb. 2021.
- [8] T. T. Nguyen, H. H. Nguyen, R. Barton, and P. Grossetete, "Efficient design of chirp spread spectrum modulation for low-power wide-area networks," *IEEE Internet Things J.*, vol. 6, pp. 9503–9515, Dec. 2019.
- [9] H. H. Nguyen and E. Shweddyk, *A First Course in Digital Communications*. Cambridge University Press, 2009.
- [10] J. Proakis and M. Salehi, *Digital Communications*. McGraw Hill, 2008.